

See discussions, stats, and author profiles for this publication at: <https://www.researchgate.net/publication/274832874>

Design, Production & Test of a Micro-Pulsed Plasma Thruster

Conference Paper · April 2012

CITATIONS

0

READS

113

2 authors:



Burak Karadag

Japan Aerospace Exploration Agency

9 PUBLICATIONS 0 CITATIONS

[SEE PROFILE](#)



Gokhan Inalhan

Istanbul Technical University

93 PUBLICATIONS 1,713 CITATIONS

[SEE PROFILE](#)

Some of the authors of this publication are also working on these related projects:



COPTRA: Combining Probable Trajectories [View project](#)



AUTOFLY-Aid: Flight Deck Automation Support with Dynamic 4D Trajectory Management for Responsive and Adaptive Airborne Collision Avoidance [View project](#)

All content following this page was uploaded by **Gokhan Inalhan** on 25 January 2016.

The user has requested enhancement of the downloaded file.

DESIGN, PRODUCTION & TESTING OF A MICRO-PULSED PLASMA THRUSTER FOR NANOSATELLITES

Burak Karadağ
Aerospace Engineering Department
Middle East Technical University
Ankara, Turkey 06800
Email: karadagb[at]yahoo.com

Assoc. Dr. Gökhan İnalhan
Controls & Avionics Laboratory
Department of Aeronautical Engineering
İstanbul Technical University
İstanbul, Turkey 34469
Email: inalhan[at]itu.edu.tr

Abstract—In this study, design, fabrication and testing of a micro-pulsed plasma thruster(μ PPT) is described. The two-stage μ PPT concept of Dr. John Schilling at AFRL, Air Force Research Laboratory, was scale-built for nanosatellites and thrust measurements was performed in order to corroborate his findings. To assess performance of the μ PPT, micro-Newton dynamic thrust measurement stand, in which impulse analysis is based on the theory of oscillations in a 1-D system, was designed and produced. Furthermore, the two-stage μ PPT was miniaturized by using off-the-shelf components and benefitting from electrolytic process. In conclusion, the thrust measurement results were issued and several advance subjects for future work was discussed.

I. INTRODUCTION

Chemical propulsion systems have not evolved much over the course of several decades. Although very high powers and thrust levels can be obtained in chemical propulsion systems, they are energy limited due to the fact that chemical reactants have certain amount of energy per unit mass. As electric propulsion systems can drive the energy generated by solar panels and/or nuclear power sources, they enable heavy payloads to be transported in space. However, electric propulsion systems can only produce very low thrusts compared to chemical ones, which means they cannot be used for space launch purposes.

Pulsed plasma thrusters(PPTs) are thrusters variation of electromagnetic electric propulsion systems. The natural properties of plasma is exploited to produce thrust and high exhaust velocities with very low fuel consumption in these systems. The first pulsed plasma thrusters was used in the Zond 2 spacecraft, launched on November 30, 1964 by the Soviet Union, for three-axis attitude control. A PPT was used aboard the LES-6 satellite for 10 years in 1968 by the United States. PPTs are utilized for onboard propulsion applications such as station keeping, attitude control, orbit transfer, drag compensation, formation flying and de-orbiting.[14]

PPTs were tested many times in space since 1964, and therefore they are flight-proven subsystems. Table 1 gives some past PPT missions.

Spacecraft	Mission
Russian Zond 2 1964	Attitude control and stationkeeping
LES 6 1968	East-West stationkeeping
TIP II/III 1975/1976	Orbit Insertion & Drag correction mnvr
LES 8/9 1976	Attitude control
NOVA 1/2 1981/1988	Orbit Insertion & Drag make-up
NOVA 3 1984	Orbit Insertion & Drag make-up
EO-1 2000	Pitch axis control and momentum mgmt
Dawgstar 2001	Attitude and orbit/formation control
FalconSAT 3 2007	Attitude stabilization

TABLE I
SOME PAST PPT MISSIONS

In the 1960s PPT was considered to be used for space-flight applications, albeit it had much lower efficiency, through its durability, development in short time, simplicity, and low cost. PPTs are classified into two major types: Rectangular(breech-fed) and coaxial(side-fed). PPTs may also be classified according to changes including short pulse vs quasi steady; ablation area; the location and type of the igniter plug; alternate propellants other than Teflon; parallel vs flared rectangular electrodes; ablating, non-ablating, and conductive nozzles; oscillatory vs non-oscillatory current; and applied magnetic field.[14]



Fig. 1. μ PPT firing in night-time

Figure 1 pictures miniaturized μ PPT firing in night-time.

There is an increasing demand for the nanosatellites to support military and civilian missions such as space-based radar and Earth observation, which needs to space-reliable

and robust thrusters capable of producing precise impulse bit and enabling fine attitude and position control. μ PPTs are one of the electric propulsion systems that can meet the need. Furthermore, as the space debris gradually proliferates, it enlarges possibility circle of Kessler syndrome, which in result threaten our opportunity to take advantage of space in future years. In order to reduce space junk, The Inter-Agency Space Debris Coordination Committee (IADC) has carried out a study regarding orbital lifetime effect on collision rate in Low Earth Orbit(LEO) and it is obtained that orbital lifetime of maximum 25 years is plausible and convenient limit[11]. Thus, another application is de-orbiting.

II. MICRO PULSED PLASMA THRUSTER (μ PPT)

The μ PPT was originally developed by Dr. Gregory Spanjers of AFRL in 1998 with the intention of reducing size and complexity of conventional PPTs[7]. Similar to a standard PPT, the μ PPT also benefits from plasma properties to generate thrust resulting in high exhaust velocities. Nevertheless, in the μ PPT design separate spark plug, trigger circuit and spring is eliminated. Besides, power requirement and thruster volume is dramatically decreased through the innovative design. Although varied fuel types may be used, solid Teflon is the most preferred one because of the fact that mechanical valves, tankage, feedlines, seals and other flow components for liquid or gas propellants reduce operational convenience and reliability.

1) *Operating Principle of The Three-Electrode Coaxial μ PPT*: Fundamentally, the Lorentz force, $F = q(E + vxB)$, is the origin of the thrust. For a given 0-15 V potential difference is increased to 0-4 kV by means of EMCO E40 high voltage converter. The potential difference of 0-4 kV is used to charge main and trigger capacitors.

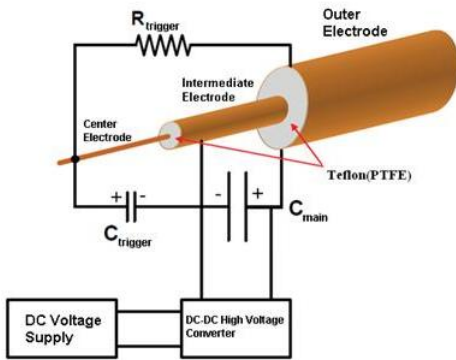


Fig. 2. μ PPT schematic [7]

Figure 2 shows μ PPT schematic.

μ PPT is initially fired between the intermediate and center electrode by a low energy breakdown. This discharge supply adequate seed ionization to allow the higher energy conduction breakdown between the intermediate and the outer electrode. The discharge between the intermediate and central electrode is termed as the trigger discharge and between the intermediate

and outer electrode is termed as the main discharge. The trigger discharge energy is generally about 1/50th that of the main discharge.[7]

The capacitors are energized as shown in Figure 3 and discharged at a certain frequency (in our case the frequency is 1 Hz). This frequency can be changed by altering the resistance of the trigger resistor. The potential difference through the discharge of trigger capacitor between cathode(the intermediate electrode) and anode(center electrode) parallel to each other, provide the seed ionization to enable higher energy conduction breakdown between center and the outer electrode. Arc discharge is formed across the surface of Teflon and some solid Teflon particles is removed, refer to the ablation.

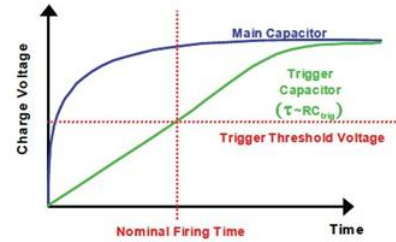


Fig. 3. Energizing the two-stage μ PPT capacitors[7]

When the power supply is on, the μ PPT circuit will begin loading capacitors as shown in Figure 3 The main capacitor is loaded to the full output voltage of the high voltage converter. To prevent discharge initiation, the threshold voltage for surface discharge initiation between the intermediate and outer electrode is well above the charge voltage on the main capacitor. When the trigger capacitor attains its threshold voltage, a discharge arc between the center and intermediate electrode will begin, and this will enable adequate seed ionization for the main discharge to be initiated.[7] By using 98 M Ω trigger resistor in the charge path the charging rate of the trigger capacitor is delayed. There is a linear correlation between input and output voltage of Emco E40 high voltage converter. In order to reach 4 kV potential difference, 15 V has to be applied to the high voltage converter[4].

Figure 4 pictures general schematic of a solid fuel μ PPT.

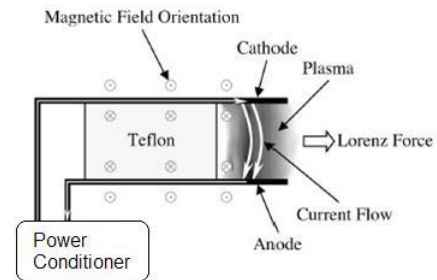


Fig. 4. General schematic of a solid fuel μ PPT[8]

The particles that is ablated from the surface of Teflon owing

to the high voltage difference enter into electric arc and ionized to plasma form. High current flow in the electric generate B magnetic field. The magnetic field and the current in the electric arc interact with each other in order to compose $\mathbf{J} \times \mathbf{B}$ the Lorentz force. This force accelerate the particles ionized and ablated from the surface of Teflon bar.

The first prototype of the μ PPT photographed in mid-discharge is shown in Figure 5.



Fig. 5. μ PPT during firing

The three-electrode design is more resistant to short-lasting augmentations in the trigger discharge starting voltage. It minimizes shot-to-shot variation of the main discharge and reduce carbonization contingency on the propellant face. Besides, the seed ionization diminishes the required voltage for the main discharge. For instance, in a 2-electrode configuration for a 0.25" diameter outer electrode up to 40 kV is required to commence the discharge while this voltage is typically 3 kV or less with the three-electrode design.[7]





	Initial State
	Arc Formation and Propellant Heating
	Ablation and Plasma Acceleration
	Late-Time Ablation, Particulate Emission, Cool-Down

Fig. 6. General operational sequence of a single pulse μ PPT

Figure 6 illustrates general operational sequence of a single pulse μ PPT.

However, it is experienced that if the trigger capacitor is removed μ PPT firing is began without any seed ionization by using only the main capacitor. In a personal correspondence

with Dr. Schilling, we are informed that atmospheric breakdowns are usually easier to initiate than surface discharges in vacuum, and also more unpredictable. Therefore, the anomalous behavior may be because of the firing in the air. The μ PPT may be fired in vacuum as a part of future experiments in order to clarify this phenomenon.

PPTs suffer from low efficiency typically between 3-8%. Propellant sublimation occurring after the main discharge, refer to the "late time ablation" is one of primary factors. This late time ablation turns out a low speed gas a macro particles that does not play a significant role in producing thrust. Evaporating the propellant requires only about 2-4% of the energy necessary for acceleration of the propellant to high speeds. All the material is not abandoning the surface. The surface continues to evaporate long after ending of the discharge pulse culminating in mass not accelerated to high speeds by electrodynamic and gas-dynamic forces. Amount of mass attending late-time ablation is not well comprehended.[14]

During the μ PPT firing erratic behaviors were observed. As it can be seen from inside the blue circles in Figure 7, the main discharge was not appearing at the end of the electrode but somewhere in the air around the thruster during firings. Firing the μ PPT in air might be the reason behind this phenomenon. It is certain that firing the μ PPT in vacuum environment is the best way to confirm. Even though firing a micro μ PPT in air is a good check for basic workmanship and functionality, for precise, repeatable results, and good performance measurements, the μ PPT is needed to be operated in a vacuum chamber.



Fig. 7. The μ PPT firing anomaly

Experiments show that certain concavity is formed on Teflon propellant area which is straight at first. It is associated with that heat transport from the arc intensifies in the center of the surface[14]. When the thruster is fired enough to ablate the first few millimeters of propellant surface, a smooth and slightly curved propellant face, smoothly rounded electrode edges, and consistent performance from the thruster was observed. This requires several thousand discharges, depending on the pulse energy used[7]. Average propellant consumption rate observed in breech-fed PPTs is in most cases lower than μ PPTs. The propellant consumption rate for the breech-fed LES 8/9 was

28 $\mu\text{g/s}$ for a 20 J, 1 Hz discharge. By linearly scaling with energy and power, the propellant consumption rate for the LES 8/9 2.7 times lower than that of μPPT [12].

Although PPTs are simply established, they include many complex interactions stem from electromagnetic and electrothermal processes[14]. Experiments by Spanjer et al. propose 40% of the mass loss from the PPT is in the shape of low-speed macro-particles which do not contribute significantly to the impulse bit[13]. Using a high area-ratio nozzle-electrode combination in a coaxial PPT can increase electromagnetic and gas-dynamic thrust components. Augmenting the nozzle size and lessening the stored energy tended to diminish I_{sp} . The anode erosion is generally 10 times more than the cathode in the case the same material is used.[14] It was deduced that the gas-dynamic forces compose 48% of the thrust, and the magnetic forces contribute 52% of it[15]. The magnetic field generated by electro or permanent magnets will improve the $j \times B$ acceleration, and the thrust[14].

A LDA in the Trisonic Research Laboratory (TRL), which is able to measure particle velocity up to 700 m/s, was tried to measure velocity of plasma particles coming out of the μPPT . However, exhaust speeds of PPTs range from 3 to 50 km/s depending on the design[14]. Despite, velocity measurement was not accomplished, it was understood that velocity of the plasma particles is bigger than 700 m/s.

2) μPPT Reproduction: The three-electrode coaxial μPPT consists of four major components below: Semi-rigid coaxial cable, high voltage capacitor, DC-DC high voltage converter, and resistor.

The first component is semi-rigid coaxial cable, generally used as a transmission line for radio frequency signals and microwaves, and commercially available on the market. In our work, we requested JYEBAO Co., Ltd to produce custom semi-rigid cable for us. This cable, known also as RF cable, is composed of three nested conductive metals and the material among these metals is politetrafluoroetilen(PTFE).

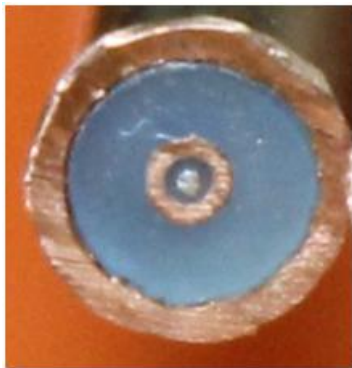


Fig. 8. Semi-rigid coaxial cable

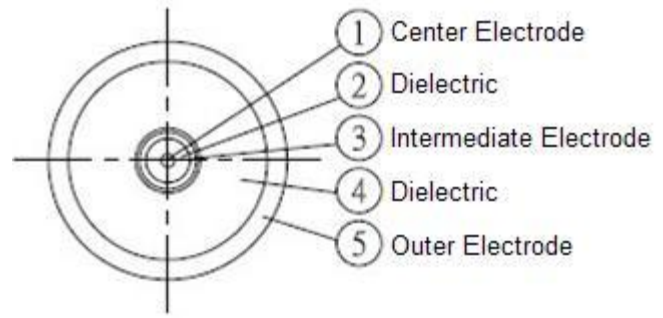


Fig. 9. Semi-rigid coaxial cable technical drawing

Figure 8 pictures front side of the μPPT Tube, Figure 9 shows the semi-rigid coaxial cable technical drawing.

The most important factor is ensuring that the maximum frequency of the cable is much greater than the frequency of the μPPT discharge. The μPPT frequency is only a few MHz, and most semi-rigid coaxial cable is designed for microwave applications at hundreds of MHz to a few GHz. This is unlikely to be a problem. Teflon, also known as PTFE is a standard insulator for semi-rigid coaxial cable, but other types of insulators for special applications may be used by manufacturers such as Micro-coax; therefore, they may not work as PPT propellants. Additionally, attenuation and insertion loss are considerable.

The second component is high voltage capacitor. The 4 kV mica capacitor[3] of Custom Electronics Inc., model number KMR1A8121SP-2, was employed. This capacitor is a combined form of two capacitors into a single unit with a common ground. The first capacitor named main capacitor has a capacitance of 0.5 μF and the second capacitor called trigger capacitor has a capacitance of 0.02 μF . The μPPT was fired at 3 kV corresponding to 2.25 W · s or Joules from the equation: $E = 0.5CV^2$. A 20 k Ω resistor was connected in series with the 98 M Ω trigger resistor to determine the capacitor voltages. During the operation the voltage of the main capacitor was measured as 1750 V and of the trigger capacitor was measured as 325 V by using a multimeter measurement device.

The third component is DC-DC high voltage converter. The Emco High Voltage Corporation's E40 converter[4] was utilized. The converter accepts voltage input of 0-15 V and return output voltage of 0-4 kV by drawing maximum 0.75 mA.

The last component is 98 M Ω 4.5 W trigger resistor was derived from 9 pieces 0.5 W 56 M Ω resistors by connecting in parallel and series. The components was assembled by soldering them together using solder wire and soldering iron .

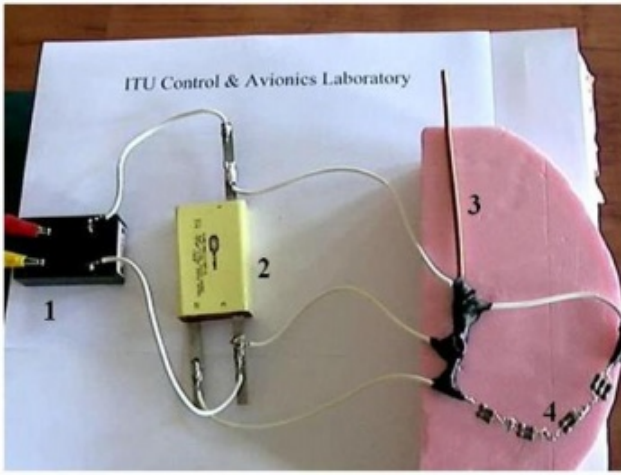


Fig. 10. Baseline μ PPT

In Figure 10:

- 1) Emco E40 high voltage converter
- 2) Custom Electronics KMR1A8121SP-2 capacitor
- 3) Semi-rigid coaxial cable
- 4) 98 M Ω Trigger resistor

Table 2 explains baseline μ PPT configuration.

Item	Property
Outer Electrode Diameter	0.35814 cm
Outer Electrode Material	Copper
Intermediate Electrode Diameter	0.08636 cm
Intermediate Electrode Material	Copper
Center Electrode Diameter	0.02032 cm
Center Electrode Material	Ag-Covered, Cu-clad Steel
Dielectric Material	PTFE
Main Capacitance	0.5 μ F
Trigger Capacitance	0.02 μ F
Trigger Resistance	98 M Ω
Power Supply	EMCO E40 4kV

TABLE II
BASELINE μ PPT CONFIGURATION

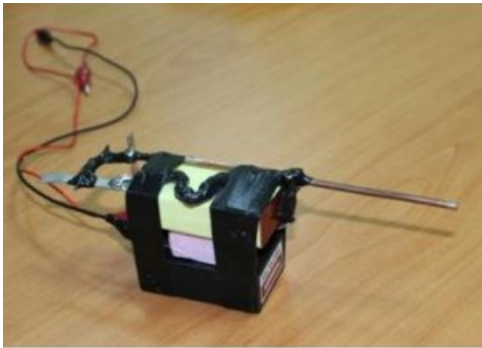


Fig. 11. Compact form of the μ PPT(without external packaging

For thrust measurement convenience at the laboratory the μ PPT was reassembled into a compact form. Figure 11 shows the first μ PPT prototype.

III. DESIGN AND PRODUCTION OF A MICRO-NEWTON DYNAMIC THRUST STAND

The idea behind the thrust measurement is that a rectangular aluminum rod oscillates when the μ PPT imparts an impulse to it. By measuring the time-dependent displacement of the rectangular aluminum rod, the impulse can be determined from the beam deflection formulae.

Figure 12 pictures concentrated load P at any point.

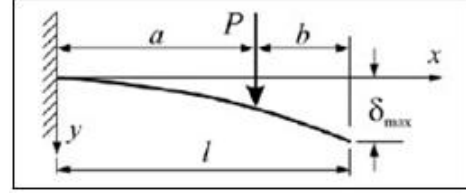


Fig. 12. Concentrated load P at any point

Deflection at Any Section in Terms of x :

$$y = \frac{Px^2}{6EI} (3a - x) \quad \text{for } 0 < x \leq a \quad (1)$$

Table 3 explains properties of aluminum beam.

Thermal expansion coefficient (20 ⁰ C-100 ⁰ C)/ ⁰ C	24x10 ⁻⁶
Modulus of elasticity (E) Kg/mm ²	7000
Specific weight Gr/cm ³	2.71
Rigidity (HB) Kg/mm ²	20
Thickness mm (b)	0.4
Width mm (h)	29
Length mm (L)	150
Distance of applied force (P) from the fixed point, x	140
Moment of inertia (I)	(hb ³)/12=58/375

TABLE III
PROPERTIES OF ALUMINUM BEAM

In order to confirm Dr. John Schilling's thrust measurements and to assess thrust level of the miniaturized μ PPT, a thrust stand[6] similar to the one in the study of Dr. Kevin Kremeyer from PM&AM Research was designed and manufactured. An eddy current sensor which has 3.9 nanometer dynamic resolution @RMS, fg=1 kHz and measuring range of 3 mm was used instead of capacitive gage since they have larger measuring range, higher resolution, and lower cost.

A. Measuring Principle of Eddy Current Sensor

The eddyNCDT 3700 measurement system is a sort of contactless displacement transducer and it functions by virtue of eddy currents on objects manufactured with a electrically conducting and non-ferromagnetic material. As alternating currents of high frequency move through a sensor coil, eddy currents in the electrically conducting measurement target are induced as shown in Figure 13 by the electromagnetic field emanates from the sensor coil. As a result, the alternating current resistance of the coil is altered. An electrical signal due to the change in impedance is delivered in parallel with the distance of the measurement target from the sensor.[1]

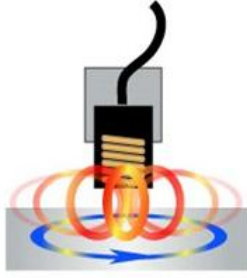


Fig. 13. Magnetic field induces eddy current in conductive target[1]

To prevent from measurement ambiguity caused by the sensor contact to the measurement target and mechanical damage to the sensor, there is a minimum space between the measurement object and the sensor must be left.[1] U3 unscreened sensor was inserted through the hole in the sensor holder and screwed tight by turning the mounting nuts on both sides on the thread.

B. Calibration

Even though the eddyNCDT 3700 measurement system come with the factory calibration, re-calibration is required if there is a change in material and geometry of the measurement target or in the sensor head. The measurement system is calibrated according to two distance points. These two reference points are the start of the measuring range SMR and the end of the measuring range EMR[8]. Therefore, a calibration device is required before performing any measurements. To this end, CMCP610 Eddy Probe Calibrator STI Vibration Monitoring Inc. with non-rotating micrometer spindle[2] was utilized. The micrometer spindle is a precise device, which give measurements in increments of 0.001 inches, and it is used to adjust needed physical gap between the sensor head and the measurement target mounted to the spindle.

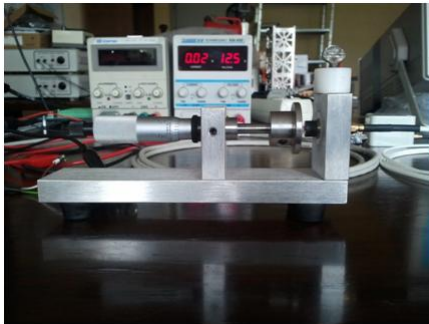


Fig. 14. CMCP610 eddy probe calibrator

Figure 14 pictures CMCP610 eddy probe calibrator.

By using the Eddy Probe Calibrator, the measurement target is put in a position that SMR is provided with regard to the sensor head. Later, the zero potentiometer for channel A is used to arrange output voltage to the desired value(in our case 0 V)[1].

Subsequently, the measurement target is placed such that EMR is provided with regard to the sensor head. After, the gain potentiometer for channel A is used to arrange output voltage to the desired value(in our case 10 V). The maximum output voltage cannot be set any higher than the maximum output voltage set at the factory[1].



Fig. 15. Single-channel system DT3701, the controller

In Figure 15, number 1 is the zero potentiometer, and number 2 is the gain potentiometer for channel A.

The sensor functionality was tested by utilizing an oscilloscope before of the μ PPT thrust measurement.

C. Micro-Newton Dynamic Thrust Stand

Testing of the μ PPT was quite challenging and entailed us to design and produce a micro-Newton thrust stand. At first, a similar electronic balance system used at the Delf University of Technology[5] was suggested for the thrust measurements. Nonetheless, although it might work we refrain from that idea because we were concerned that such a balance would not accurately measure brief, pulsed thrusts as balances are designed to read steady force/weight. If a balance manufacturer confirms that their electronic balances are reliable for pulsed measurements, it is certainly worth trying it. In addition, sampling rates of any available strain gage and accelerometer was well in excess of the required sampling rates in order to properly measure the μ PPT dynamic thrust.

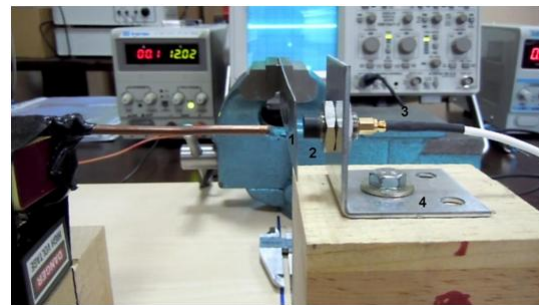


Fig. 16. Thrust stand close view

Figure 16 illustrates micro-Newton dynamic thrust measurement stand from different angle.

In Figure 16:

- 1) The rectangular aluminum rod
- 2) Sensor head
- 3) Sensor cable
- 4) Bracket

In a personal correspondence with Mr. Johann Mueller from Micro-Epsilon Messtechnik GmbH & Co. KG, we are noticed that in order to get nanometer or sub-nanometer resolution it is important to use an excellent linear regulated power supply and a low pass filter. This is much more important than the material. Besides, small temperature measurements can also throw off the calibration of whatever instrument to measure thrust, and at the micro-Newton range this can be significant.

$$\Delta T = \frac{\Delta L}{\alpha L} = \frac{3.9 \times 10^{-9}}{12 \times 10^{-6} \times 2 \times 10^{-4}} = 1.625 \text{ }^{\circ}\text{C} \quad (2)$$

Where, α : Thermal expansion coefficient of iron ΔL : Dynamic resolution of the eddy current sensor L : Thickness of the bracket made of iron

For this reason, the room temperature at which thrusts measurements are performed should not change more than 1.625 $^{\circ}\text{C}$ not to get erroneous measurements.

Voltage (V)	Displacement (mm)
9.995117	0
8.9956053	0.300146562
7.9960936	0.600293123
6.9965819	0.900439685
5.9970702	1.200586246
4.9975585	1.500732808
3.9980468	1.80087937
2.9985351	2.101025931
1.9990234	2.401172493
0.9995117	2.701319054
0	3.001465616

TABLE IV
VOLTAGE VS. DISPLACEMENT

Displacement (mm)	Thrust (μN)
0	0
1	11234.86683
2	22469.73366
3	33704.60048

TABLE V
DISPLACEMENT & THRUST CORRELATION

Table 4 was formed by simply dividing 0-9.995117 interval into equal pieces and calculation by using Equation 1 resulted in Table 5. Both of them was used to convert voltage values to actual thrust values of the system.

Although the eddy current sensors are calibrated in the factory, they might need field calibration since room temperature, moisture ratio and other factors might differ. To realize whether or not our eddy current sensor needs calibration, output voltage values was examined while the sensor was at SMR and EMR. When the sensor was at SMR, output voltage was 0.659180 Volt and when the sensor was moved

at EMR, output voltage was 9.111328 Volt, which means the sensor was needed to be calibrated. By simply turning the zero potentiometer until the output voltage becomes 0 V while the sensor is at SMR, and the gain potentiometer until the output voltage becomes 9.995117 V while the sensor is at EMR, the maximum voltage. In spite of our expectations from the eddyNCDT 3700 sensor manual, it does not reach to 10 V how much the gain potentiometer is turned.

In order to read analog inputs, NI PCI-6024 card and NI BNC-2110 shielded connector block was exploited. Besides, National Instruments Labview 2010 Software was utilized to register time-voltage values in a single text file.

D. Thrust Measurement Results

Thrust measurements were performed on the baseline two-stage μPPT at a nominal energy of 2.25 J at 1 Hz. It is prominent that if the μPPT is fired continuously in our thrust stand, successive thrust vectors will be united and cause rectangular aluminum rod to be moved more than it actually will due to a single pulse. As overlapping is definitely going to change our data outcome, single pulses were only recorded.

The voltage difference delta V is proportional to the thrust produced by the μPPT . The largest observed thrust was of 296.3745 micro-Newton and the smallest one was of 32.92862 micro-Newton during measurements.

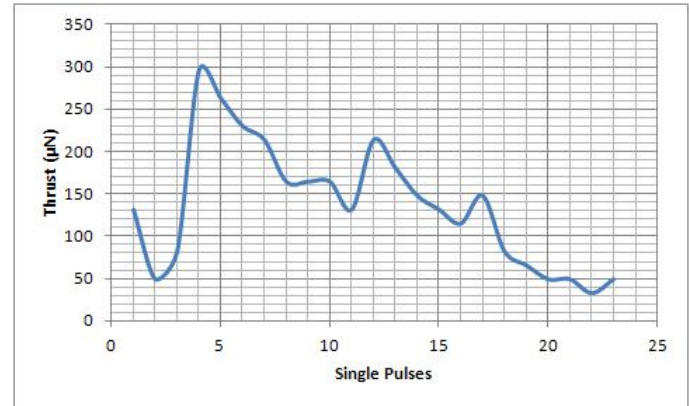


Fig. 17. Overall the μPPT performance

However, it is obvious from Figure 17 that there are sharp thrust variations among the single pulses. Changing amplitudes of the sound waves dispersed during the firings is also an indicator of this fact. The stored energy alterations in the capacitors may be one of the reasons behind this phenomenon.

In addition, since the propellant surface withdraws within the outer electrode, viscous losses are ascended. This is more likely to be culminated in thrust declination along the thruster life. Recessing of the propellant face inside the electrode structure brings about essential viscous losses. The more the propellant face recesses, the more Teflon particles in plasma form will travel inside the cylindrical copper electrode structure. When the plasma particles moves in it they will collide with its wall and decelerate. Since acceleration is the

major thrust generating element, as the traveling duration in the copper electrode structure increases, the thrust obtained will be reduced over the thruster life.[7]

IV. μ PPT MINIATURIZATION

Mini-thrusters could make it easier for the small satellites to fulfil space maneuvers and proceed challenging tasks such as searching for new planets. The μ PPT prototype is unnecessarily heavy, each package weighs more than 250 grams, to be deployed on cubesats and nanosats. Therefore, it is desired to reduce the mass of the propulsion unit as much as it is possible.

A. Thinned Outer Electrodes

The outer electrode thickness constitutes majority of the μ PPT propellant tube mass and has nothing directly to do with thrust generation.

If the electrode thickness is more than the thickness required to keep resistive heating small respect to other efficiency losses in the structure of the electrode, there is wasted electrode mass. The important consideration is that ablation of the outer electrode should be roughly at the recession rate of the propellant not to cause the thruster to fail.[7]

Although there are several ways of copper thinning process. The semi-rigid coaxial cable was immersed into concentrated solution of Copper II Sulfate Pentahydrate not to end up with toxic fumes, such as in case of nitric acid or sulphuric acid. The outer electrode of the μ PPT tube is attached to the positive pole of the power supply and a copper plate is attached to the negative pole. The copper mass that move to the negative end can be calculated according to the Faraday's laws of electrolysis.

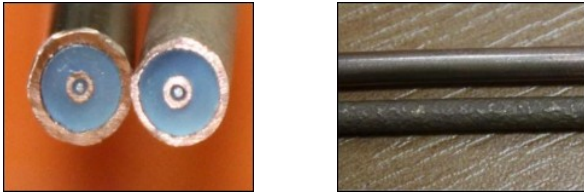


Fig. 18. Before(left) and after(right) electrolysis

A few μ PPT tubes exposed to electrolysis process to reduce the outer wall thickness. Size and mass of electrodes was reduced by using electrolytic process.

Figure 18 indicates outer wall thickness difference. Outer electrode diameter reduced from 3.5814 mm to 3.54 mm, 3.34 mm and 3.20 mm. As it can be seen from Figure 18 mitigation of the copper was not uniform. The resulting μ PPT proved functionality at all of these wall thicknesses.

B. Smaller and Lighter Components

The components, capacitors and high voltage converter, were the heaviest components, so they were altered with off the shelf very lighter ones. The first component is Emco QH40-15R high voltage converter which weighs only 4.25 grams. The converter accepts voltage input of 0-15 V and

return output voltage of 0-4 kV by drawing maximum 0.313 mA. In addition, several high voltage capacitors were tried out. The second component is polypropylene film 0.47 μ F Cornell-Dubilier 2 kV capacitor, model number is 940C20P47K-F, and metallized polypropy 0.022 μ F Genteq 3 kV capacitor, part number is 42L4223.

A smaller micro-pulsed plasma thruster, which weighs 62 grams without external package, was obtained. In addition, the μ PPT was packaged by exerting 1 mm-thick Aluminum sheet in order to protect it from unwanted shocks and heat. The packaging operation increased 177 grams the weight of the unpacked structure. Figure 20 shows both μ PPT.

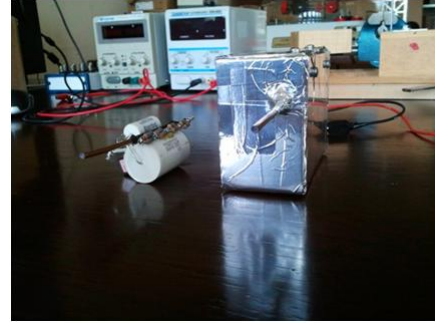


Fig. 19. Both μ PPT

V. FUTURE STUDIES

There are many future studies needs to be performed about μ PPTs.

A. Thermal Vacuum Chamber

In order to benefit from μ PPTs in space for varied missions from precise attitude control to main propulsion system, they are firstly needed to be fully tested on the ground. Functional tests on a μ PPT at a wide range of pressures should be fulfilled in a chamber capable of high vacuum, between 10^{-2} Torr and 10^{-7} Torr.

As atmospheric or near-atmospheric conditions provoke oxidation on the PPT, high vacuum condition is required in thermal vacuum chamber. The thruster is likely to arcing which is out of hand if the PPT is performed at pressure higher than 1.3 pascals (0.01 torr). As condense air particles make available the current uses diverse routes. This leads to arcing not at the electrode tip but at other spots.[9] Nonetheless, we frequently operated the thrusters in open air for basic functional tests and never saw problems with oxidation and it did not any harm to operate the μ PPT at higher pressures.

Additionally, effect of vibrations in the thrust chamber should be taken into account as the performance measurements will be affected.

B. Alternative Propellants

By constructing a different design, the force obtained thermodynamically might increase thrust power ratio of the PPT with the help of the chemical energy stored in the propellants. For instance, the thrust power ratio is increased

using hydroxylterminated polybutadiene-ammonium perchlorate (HTPB-AP)-based propellants compared to the case of ordinary Teflon[10]. However, it should be considered that conventional PPT designs early in their lives are not able to promptly employ thrust by gas-dynamic operation which is generated by chemical augmentation[7].

C. Plume Studies

As an undesired disadvantage of μ PPTs, plume of μ PPTs may cause substantial problems with sensors and power generation. The exhaust plume consisting of solid teflon particulate may accumulate on solar array surfaces and limit the satellite lifetime and mission capacity. For example, pictures from high resolution camera on a military surveillance satellite may be blurred due to the plume. Thus, in order to comprehend these contamination issues, the exhaust plume characterization is needed to be detailed.

D. Modeling and Simulation

Mathematical and numerical models are a widely accepted way of investigating PPT characteristics. It is necessary to develop theoretical modeling so as to enhance performance and control of PPTs. PPT behavior in many modern computer simulations of still depends on empirical formulations of mass ablation and vaporization due to using sophisticated Magneto-Hydro-Dynamic(MHD models such as MACH2 to explain the arc formation and plasma acceleration processes. In spite of the extensive simplifications, considered as one-dimensional or two dimensional, in existing computational PPT models, a study regarding the development and numerical implementation of a more accurate solid fuel ablation model for PPTs should be carried out.[8]

In addition to studies mentioned, different sized and two axis semi-rigid coaxial cables such as Pasternack PE-047SR and Pasternack RG401U, and nozzles may be tried to examine their affects on the thrust output. It would also be preferred to connect multiple μ PPTs to a single power supply so as to fire any desired thruster and reduce total thruster mass by using high voltage switch circuit design.

VI. CONCLUSION

In this study, first of all, a literature survey regarding Pulsed Plasma Thrusters is achieved. In addition to past PPT works, fundamental principle of operation of PPTs and μ PPTs is clarified. Dr. John Schilling's the two-stage μ PPT concept is expressed. After identification of its components, the two-stage μ PPT concept is assembled. Subsequent to regeneration of the two-stage μ PPT concept, its functionality is confirmed by accomplishing firing in the air.

Secondly, some physical characteristics of PPTs is addressed and a LDA experiment is carried out in order to confirm one of them, exhaust velocity. Following, production of smaller and lighter μ PPT prototype, aims to reduce the weight of the μ PPT, is mentioned. Subsequently a detailed description of our micro-Newton dynamic thrust measurement stand is issued. Apart from explanation of working principle of

the micro-Newton dynamic thrust measurement stand, thrust performances of the first and second μ PPT prototypes are determined and compared.

Finally, a μ PPT model, which is the first electric propulsion system made in Turkey, was developed and tested to be used in ITU PSAT II nanosatellite for three-axis active attitude control.

ACKNOWLEDGMENT

We'd like to thank to The Scientific and Technological Research Council of Turkey (TÜBİTAK) as this work is partially funded under TÜBİTAK 108M523 Project.

REFERENCES

- [1] Micro-Epsilon Messtechnik GmbH & Co. KG eddyNCDT 3700 instruction manual
- [2] STI Vibration Monitoring Inc. CMCP610 eddy probe calibrator data sheet
- [3] Custom Electronics Inc. KMR1A8121SP-2 data sheet
- [4] Emco High Voltage Corporation E40 data sheet
- [5] Mettler balance thrust measurement. Retrieved on July 18, 2011 from <http://www.lr.tudelft.nl/live/pagina.jsp?id=c73f2191-0534-4333-a8b7-d53327416fcf&lang=en>
- [6] Kremeyer, K., Lapeyre, J., and Hamann, S., *Compact And Robust Laser Impulse Measurement Device, With Ultrashort Pulse Laser Ablation Results*, Fifth International Symposium on Beamed Energy Propulsion. AIP Conference Proceedings, Volume 997, pp. 147-158 (2008).
- [7] Schilling, J., *Development of The Two-Stage Micro Pulsed Plasma Thruster*, Ph.D. Thesis University of Southern California, 2007.
- [8] Stechmann, P. D., *Numerical Analysis of Transient Teflon Ablation in Pulsed Plasma Thrusters*, Worcester Polytechnic Institute, 2007.
- [9] Debevec, H. J., *Vacuum Chamber Construction And Contamination Study Of A Micro Pulsed Plasma Thruster*, United States Air Force Institute Of Technology, 2006
- [10] Hideto Mashidoria, H., Kakamib, A., Muranaka, T., & Tachibana, T., *A Coaxial Pulsed Plasma Thruster Using Chemical Propellants*, Kyushu Institute of Technology, 2006
- [11] IADC Presentation to 40th UN COPUOS STSC (40th Session of the Scientific and Technical Subcommittee United Nations Committee on the Peaceful Uses of Outer Space)
- [12] Spanjers, G. G., Bromaghim, D. R., et al, *AFRL MicroPPT Development for Small Spacecraft Propulsion*, 38th AIAA/ASME/SAE/ASEE Joint Propulsion Conference & Exhibit, Indianapolis, Indiana, 7-10 July 2002.
- [13] Spanjers, G. G., Lotspeich, J.S, McFall, K.A., and Spores, R. A., *Propellant Losses Because of Particulate Emission in a Pulsed Plasma Thruster*, Journal of Propulsion and Power, Vol. 14, No.4, 1998, pp.554-559.
- [14] R. L. Burton, P. J. Turchi, *Pulsed Plasma Thruster*, J. Prop. Power, Vol. 14, No. 5, 1998, pp. 716-735.
- [15] Thomassen, K. I., and Tong, D., *Interferometric Density Measurements in the Arc of a Pulsed Plasma Thruster*, Journal of Spacecraft and Rockets, Vol. 10, No. 3, 1973 pp.163,164